Generalized cuprate gap symmetry and higher *d*-wave harmonics: Effects of correlation length, doping, temperature, and impurity scattering

David Parker,[1] Stephan Haas,[2] and Alexander V. Balatsky[3]
[1]*Max-Planck Institute for the Physics of Complex Systems, Nöthnitzer Strasse 38, D-01187 Dresden, Germany*
[2]*Department of Physics and Astronomy, University of Southern California, Los Angeles, California 90089-0484, USA*
[3]*Theoretical Division, MS-B262, Los Alamos National Laboratory, Los Alamos, New Mexico 87545, USA*
(Received 22 May 2007; published 10 September 2007)

Although $d_{x^2-y^2}$ gap symmetry is well established for the hole-doped cuprates, and for at least a portion of the electron-doped cuprates, the possibility of higher-harmonic gap functions remains. Here we analyze the higher-harmonic problem within a spin-fluctuation-mediated pairing framework by solving the BCS gap equation on a quasicylindrical Fermi surface, explicitly considering deviations from a cylindrical Fermi surface, with specified band structure. We find a number of interesting effects: the shape of the gap function is virtually insensitive to the value of the correlation length assumed; the gap near the node gets *steeper* with underdoping, implying a flatter density of states; the higher-harmonic components show a complex doping dependence; and the shape of the gap function is insensitive to impurity scattering in the unitary and Born limits.

DOI: 10.1103/PhysRevB.76.104503 PACS number(s): 74.72.Hs, 74.20.Rp

I. INTRODUCTION

d-wave ($d_{x^2-y^2}$) pairing in the optimally doped high-T_c cuprates was established in the mid-1990s through a number of experiments: Josephson interferometry,[1] tricrystal experiments,[2] various thermodynamic measurements indicating nodal superconductivity,[3–5] and Andreev spectroscopy work.[6] More recent tricrystal work[7] suggests the predominance of this symmetry over a wide range in doping. Despite the robustness of these experimental data,[8] the possibility of higher-harmonic gap functions remains. The phase-sensitive experiments suffice to demonstrate a π change in the order parameter phase for quasiparticles moving parallel to the *a* and *b* axes. However, appropriate higher-harmonic gap functions would show the same π phase change. Much past work[4] has indicated a low-temperature density of states linear in energy near $E=0$. While not entirely excluding higher-harmonic gap functions, this work has been taken as supportive of $d_{x^2-y^2}$ superconductivity.

Previous work on higher-harmonic gap functions[12] studied the effect of extended gapless regions in the cuprates induced by higher harmonics through solution of generalized Abrikosov-Gorkov equations. Ghosh[13] examined $s+d$ pairing in the cuprates in a generalized harmonic context, while Bang *et al.*[14] employed a higher-harmonic model to account for several anomalous properties of the superconductivity observed in the heavy-fermion material $CeRhIn_5$.

Two angle-resolved photoemission spectroscopy (ARPES) studies[15,16] on underdoped $Bi_2CaSr_2Cu_2O_{8+\delta}$ (BSCCO) have depicted a gap structure significantly flatter near the node than the pure *d*-wave gap. Mesot *et al.*[16] found evidence for a gap function with an 8–12 % higher-harmonic $[\cos(6\phi)]$ content, while Borisenko *et al.*[15] found the leading edge gap to contain an approximate 21% $\cos(6\phi)$ content. Within the BCS theory, such gap structures will tend to produce low-energy densities of states (DOSs) that are enhanced relative to that expected for a pure *d* wave [for which $N(E) \simeq E/\Delta$].

It is therefore most surprising that recent tunneling work[17] on underdoped BSCCO found a low-energy DOS which, while not implying a fully gapped order parameter, is substantially *depleted* relative to the pure *d*-wave case. One hypothesis consistent with these data is the use of a gap function steeper near the nodes by including higher harmonics. Since, as will be shown later, the clean-limit low-energy density of states and gap slope at the node are inversely proportional[18] a steeper gap function would yield a depleted low-energy density of states.

Given the conflicting data in this area, what we have done is to solve the BCS gap equation assuming a spin-fluctuation-mediated pairing mechanism and study the evolution of the gap function throughout the entire phase diagram of the cuprates, from the hole-doped cuprates (overdoped to underdoped) through to the electron-doped cuprates. We have also studied the effect of correlation length, temperature, and impurity scattering within the unitary and Born limits. We have not attempted to include the effects of the intervening antiferromagnetic state near zero doping; our purpose is to study the effect of these several quantities on order parameter symmetry.

II. MODEL

We begin with the spin fluctuation pairing mechanism proposed by Monthoux, Balatsky, and Pines:[19]

$$H_{int} = \frac{1}{V}\sum_{\mathbf{q}} g(\mathbf{q})\mathbf{s}(\mathbf{q})\cdot\mathbf{S}(-\mathbf{q}) \tag{1}$$

where

$$\mathbf{s}(\mathbf{q}) = \frac{1}{2}\sum_{\alpha,\beta,\mathbf{k}} \psi^{\dagger}_{\alpha,\mathbf{k}+\mathbf{q}}\sigma_{\alpha,\beta}\psi_{\mathbf{k},\beta} \tag{2}$$

with $\mathbf{S}$ the spin-fluctuation operator whose correlation function is modeled by the susceptibility

$$\chi(\mathbf{k}-\mathbf{k}',\omega) = \frac{1}{\xi^{-2} + (\mathbf{k}-\mathbf{k}'-\mathbf{Q})^2 - i\xi^{-2}\omega/\omega_{sf}} \tag{3}$$

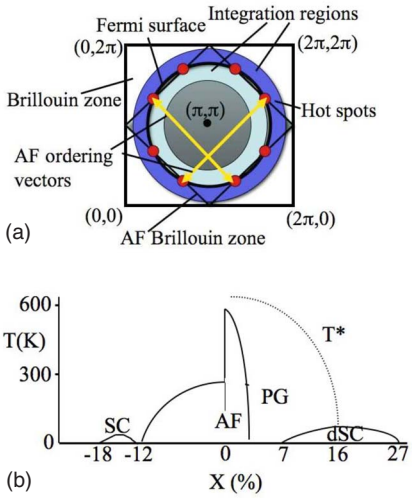

FIG. 1. (Color online) Top: Schematic diagram of the Fermi surface integration used to solve the gap equation. Note the hot spots and ordering vectors. Bottom: Schematic phase diagram of the electron- and hole-doped cuprates.

$$= \frac{\chi_0}{1 + \xi^2(\mathbf{k} - \mathbf{k}' - \mathbf{Q})^2 - i\omega/\omega_{sf}}, \tag{4}$$

where ξ is the antiferromagnetic correlation length, ω_{sf} is the spin fluctuation frequency, χ_0 is the long-wavelength limit of the susceptibility ($\propto \xi^2$), and the ordering vector $\mathbf{Q} = (\pm\pi/a, \pm\pi/a)$. The ξ^{-2} in the denominator of the first equation follows from dimensional grounds, yielding $\chi_0 \propto \xi^2$. We note that, in general, ξ, ω_{sf}, and χ_0 will depend on the doping level.

Use of the above susceptibility leads to the following BCS weak-coupling gap equation for the superconducting order parameter (like Monthoux *et al.*, we neglect the imaginary part of the susceptibility):

$$\Delta(\mathbf{k}) = \int g \frac{d^2\mathbf{k}'}{(2\pi)^2} \frac{\mathrm{Re}[\chi(\mathbf{k} - \mathbf{k}', E_k)]\tanh(E_{k'}/2T)\Delta(\mathbf{k}')}{2E_{k'}} \tag{5}$$

where $E_{k'} = \sqrt{(\varepsilon_{k'} - \mu)^2 + \Delta^2(\mathbf{k}')}$, μ is the chemical potential, and $\varepsilon_{k'}$ represents the tight-binding quasiparticle dispersion, which we take as

$$\varepsilon_{k'} = -2t(\cos k_x' + \cos k_y') + 4t' \cos k_x' \cos k_y' - 2t''(\cos 2k_x' + \cos 2k_y') \tag{6}$$

with $t, t', t'' > 0$. We have taken the coupling constant g to be 2.0 for all calculations, as in Ref. 20, with no doping dependence. In many problems of this kind the above integral is taken over the entire Brillouin zone, implying a $\Delta(\mathbf{k})$ that must be solved over an entire octant of the Brillouin zone. However, for calculational simplicity our approach, shown in Fig. 1, is to treat the interaction as relevant only in a strip of finite width around the Fermi surface, as in the original BCS approximation,[21] and assume that the order parameter depends only on the angle on the Fermi surface, not the distance from the Fermi surface. This greatly facilitates the numerical calculations necessary to solve the gap equation, particularly for large correlation lengths, which require a very fine mesh in the momentum integration variables. (For shorter correlation lengths, we have found excellent agreement between the results of our approximation and those of a full two-dimensional calculation.) However, we retain the quasiparticle dispersion and choose an integration strip of sufficient width (typically $|k_\perp'| \leq 0.6$) that the essential two-dimensional character of the problem is retained.

For all calculations we have taken t' to be 0.22 and $t'' = 0.1$, consistent with ARPES data[22,23] on $La_{2-x}Sr_xCuO_4$ (LSCO) and other published work on this issue. For simplicity, for all the calculations we have simply set $\omega_{sf} = \infty$ so that we are effectively studying the static limit. We note that, by using the actual Fermi surface determined by the quasiparticle dispersion ε_k, we no longer use the approximation of a cylindrical Fermi surface. To treat the integration properly we define new variables $k_\parallel = (k_x - k_y)/\sqrt{2}$ and $k_\perp = (k_x + k_y)/\sqrt{2}$ and exploit the fourfold symmetry of the Fermi surface, integrating along $k_\parallel$ (essentially along the Fermi surface) and across $k_\perp$ (crossing the Fermi surface). Since the Fermi surface is not square, in this approximation $k_\perp$ is not exactly perpendicular to the Fermi surface, but for most of the Fermi surface this does not introduce significant error, and near the antinodal points (where $k_\perp$ and the normal to the Fermi surface are at significantly different angles) we simply expand the $k_\perp$ integration range so that the integration is still effectively performed over a region of constant width inside and outside the Fermi surface. To avoid double counting we have restricted the integration range to be inside a single Brillouin zone.

We have assumed symmetries consistent with *d*-wave higher-harmonic gap symmetry; the gap vanishes along the directions along the Brillouin zone diagonals and is antisymmetric upon reflection about these diagonals. We have not explored the possibility of other pairing symmetries emerging as the hot spots move down the zone diagonals with underdoping, as was examined in Ref. 20.

Finally, we note that for the orthorhombic material $YBa_2Cu_3O_{6+x}$ (YBCO), there is substantial evidence for a mixed, $s+d$ order parameter, based on tunneling spectroscopic[24,25] and phase-sensitive measurements,[26] with the *s* component approximately 10–20 % as large as the *d* component. Such an *s* component is expected on the basis of simple group theory,[26] as the orthorhombicity breaks the square symmetry of the CuO planes. In this work we do not consider such mixed $s+d$ symmetries, but simply focus on the generalized *d*-wave symmetry of a spin-fluctuation pairing scenario.

III. RESULTS

A. Gap symmetry and correlation length

Depicted in Figs. 2 and 3 is one main result of this paper. These figures show the gap functions obtained for both hole-doped and electron-doped cuprates by solving the gap equation for various values of the correlation length ξ (in units of the lattice constant *a*). The figures depict a strong relation-

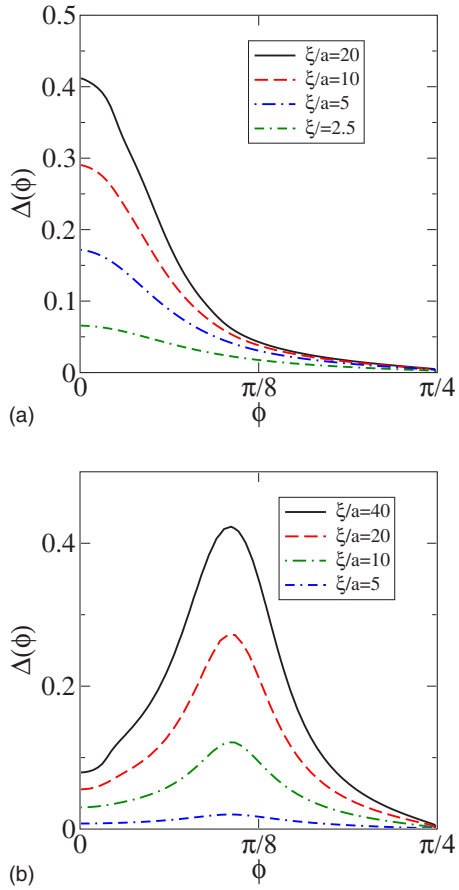

FIG. 2. (Color online) Gap amplitudes, solved within a spin-fluctuation scenario, for (a) hole-doped ($\mu=-1.2$, $n_h=0.30$) and (b) electron-doped ($\mu=-0.4$, $n_e=0.03$) cuprates.

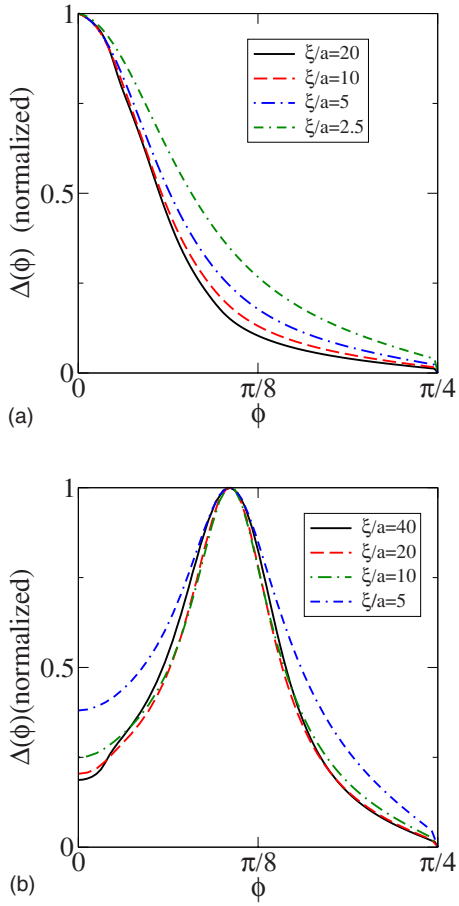

FIG. 3. (Color online) Normalized gap amplitudes for (a) hole-doped and (b) electron-doped cuprates; parameters as in Fig. 2.

ship between the correlation length and the amplitude of the gap function; longer correlation lengths are associated with larger gap amplitudes. This is not surprising given the assumption that χ_0 varies $\propto\xi^2$. Upon dividing the real part of the susceptibility by ξ^2, one finds in the denominator a broadening factor which is proportional to ξ^{-2}, so that the susceptibility grows as ξ grows.

However, the *shape* of the gap functions in Fig. 3 (obtained by simply scaling the gap functions by their maximum value) shows comparatively little dependence on ξ. These counterintuitive results are a direct result of performing an essentially two-dimensional calculation, and can be explained as follows. In two dimensions, the relevant integral in momentum space that determines the gap function has the form

$$I = \int \frac{d^2\mathbf{q}}{\xi^{-2} + (\mathbf{q} - \mathbf{Q})^2}. \tag{7}$$

Simple power counting in $\mathbf{q}$ shows that the integral depends on the cutoff momentum, so that the hot spots, while significant, do not contribute the majority of the pairing interaction. Another way to see this is to note that the hot spots are most effective in a region of momentum space of radius ξ^{-1}. Plugging this into the expression for I, and integrating over the interior of a circle of this radius, we find that the absolute contribution of the hot spot to I is independent of correlation length, while clearly I is a strongly increasing function of ξ. The *relative* contribution of the hot spot to the pairing potential therefore decreases sharply with increasing correlation length, so that there is little reason to expect a significantly sharper gap function as ξ increases.

B. Doping effects

An additional factor affecting the structure of the gap is that of doping. As one moves down the phase diagram from optimally hole doped toward underdoped, and on to electron doping, the size of the relevant Fermi surface centered at (π,π), as in Fig. 1, shrinks and the hot spots move down the antiferromagnetic (AF) Brillouin zone (BZ) diagonal. An important question to answer is the following: How does the slope of the gap near the node change with doping? Based on the motion of the hot spots down the zone diagonals, one would expect that the slope of the gap (relative to its maximum value) would increase with underdoping, while one might expect that the increase in correlation length with underdoping would flatten the gap near the node. There is therefore a competition between these two factors.

To answer this question, we have performed a calculation at various dopings, assuming that the correlation length varies in direct proportion to the distance between hole

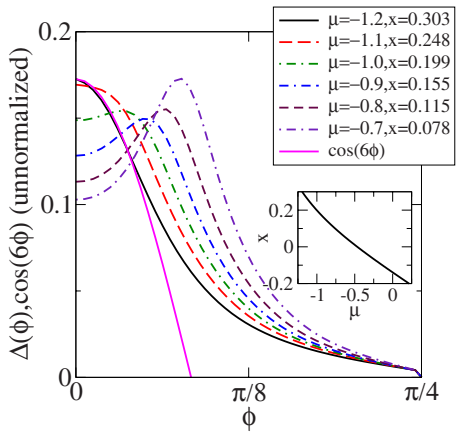

FIG. 4. (Color online) Gap amplitudes for varying doping. Correlation lengths varied as described in text. Inset: Doping–chemical potential relationship.

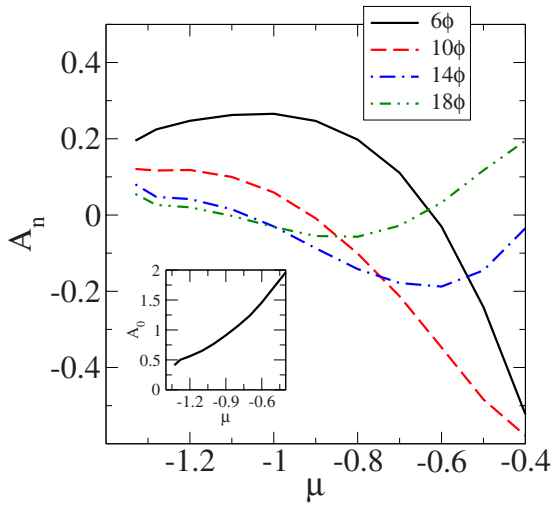

FIG. 5. (Color online) Higher-harmonic content of the gap function at various chemical potentials is shown. Inset: Coefficient of the $\cos(2\phi)$ term. Coefficients defined such that $\Sigma_n A_n = 1$.

dopants.[27] In general, this distance is $\propto 1/\sqrt{x}$, with x the hole doping. For these calculations, the correlation length ξ varied from $5a$ for the $\mu=-1.2$ case to $10a$ for the $\mu=-0.7$ case. We see at once in Fig. 4 that as the hot spots move down the AF BZ diagonals, the gap function becomes significantly steeper near the nodes. The increasing correlation length with underdoping has very little impact on gap shape, even near the nodes. It is easily shown that this greater slope leads to depleted low-energy quasiparticle density of states.[18] Here we have parametrized the angular dependence of the order parameter by $f(\phi)$:

$$N(E/\Delta) \equiv N(x) = \mathrm{Re}\left\langle \frac{x}{\sqrt{x^2 - f^2(\phi)}} \right\rangle. \tag{8}$$

For $x \ll 1$ only those values of f near 0 will contribute to the integral, and we may expand f around the node:

$$f = \nu_\Delta(\phi - \phi_0) \tag{9}$$

yielding

$$N(x) \propto \int \frac{d\phi\, x}{\sqrt{x^2 - \nu^2(\phi - \phi_0)^2}} \tag{10}$$

$$= \int_0^{x/\nu} \frac{d\phi\, x}{\sqrt{x^2 - \nu^2\phi^2}} \tag{11}$$

$$= \frac{x}{\nu} \sin^{-1}\left(\frac{\nu\phi}{x}\right)\Bigg|_{\phi=0}^{\phi=x/\nu} \propto \frac{x}{\nu}. \tag{12}$$

We see that the slope of the gap near the node and the low-energy density of states are inversely proportional, so that as the hot spots move down the zone diagonals, the low-energy density of states is depleted, in qualitative agreement with the data of Vedeneev and Maude[17] on underdoped BSCCO.

We have checked that, with the inclusion of a finite spin-fluctuation frequency (taking $\omega_{sf}=0.1t$), the gap function still steepens near the node with underdoping; this tendency, however, is weakened. A full assessment of this issue, including the doping dependence of ω_{sf}, would require a much more elaborate calculation[28] which is beyond the scope of this paper.

We also note that the maximum in the order parameter moves away from the "antinodal" point with underdoping. This is a direct consequence of the motion of the hot spot down the antiferromagnetic BZ diagonal as the Fermi surface [centered at (π,π); see Fig. 1(a)] shrinks with underdoping.[20] As stated earlier, it is possible that with sufficient underdoping into the electron-doped cuprates, another pairing symmetry becomes energetically[20] favorable; we have not considered this here.

C. Evolution of higher harmonics with doping

In general, one may write down an expansion of $\Delta(\mathbf{k})$ in higher harmonics as follows:

$$\Delta(\mathbf{k}) = A_0 \cos(2\phi) + A_1 \cos(6\phi) + \cdots. \tag{13}$$

This is the most general expansion consistent with the symmetry of the d-wave order parameter [i.e., even parity, vanishing at $\phi=(2n+1)\pi/4$ and antisymmetric around these nodal points]. Previous studies[12,15,16] have focused on the evolution of the first higher harmonic (the 6ϕ term) with impurity scattering and doping, and it is generally thought that the proportion of this harmonic increases as one reduces doping from the optimally hole-doped cuprates. Here we show that, within a spin-fluctuation model, a more complex behavior exists, while the proportion of still higher harmonics [$\cos(10\phi)$ and higher] varies with underdoping. To study this issue, we Fourier-transform the gap functions determined as a function of doping, normalized to unity at the maximum amplitude. The coefficients are defined such that the sum of the coefficients, including the main 2ϕ term, is unity. Figure 5 shows the coefficients of the various terms in the Fourier expansion at several doping levels. As the plot indicates, the magnitude of the $\cos(6\phi)$ term at first increases, as one moves from the optimally doped regime toward the underdoped. However, it then begins to decrease,

and its amplitude is approximately zero at a chemical potential of approximately −0.6. From there, the coefficient grows steadily more negative, reaching about −0.5 at the last point modeled. This is in qualitative agreement with the ARPES data[15,16] on BSCCO and the electron-doped cuprate $Nd_{2-x}Ce_xCuO_4$ (NCCO),[29] which show a 6ϕ term content rising from 0 at underdoping to approximately 0.25 at optimal doping, and falling to approximately −0.43 for NCCO.[29] Concomitantly, in our model, the magnitudes of the $\cos(10\phi)$, $\cos(14\phi)$, and $\cos(18\phi)$ terms initially decrease with underdoping, and the 14ϕ and 18ϕ terms later increase.

The rather complex, unexpected behavior of the expansion coefficients can in fact be explained rather easily, based upon the motion of the hot spots with underdoping (we use the term loosely here to include all dopings less than optimal, including the "negative" dopings of the electron-doped cuprates). The hot spots move because the Fermi surface shrinks with underdoping, as indicated in Fig. 1 of Ref. 20.

Superposed onto Fig. 4 is a plot of the gap harmonic $\cos(6\phi)$. We see that, for $\mu=-1.2$, the maximum of the order parameter is still at $\phi=0$, while $\Delta(\mathbf{k})$ drops rather rapidly away from the maximum. It is only a third of its maximum value at the first nodal point $(\pi/12)$ of $\cos(6\phi)$, and continues to decrease thereafter. Given that the Fourier coefficient $a_{6\phi} \propto \int \Delta(\phi)\cos(6\phi)$, it is clear that when the hot spot (coinciding with the maximum of the gap function) is at $\phi=0$, this coefficient will be positive. As the hot spot moves to the right, the coefficient first increases slightly, as more area is gained on the right-hand side by the motion of the gap function than is lost on the left. It then reaches a maximum and begins to fall, as increasing portions of the gap function begin to lie in regions where $\cos(6\phi)$ is negative. Ultimately, the peak in the gap function begins to lie in the region between $\phi=\pi/12$ and $\pi/4$, where $\cos(6\phi)$ is negative, and it is at this point that the coefficient becomes negative, while its magnitude increases steadily. This picture also implies that at sufficient underdoping, as the hot spot moves toward $\pi/8$, the coefficient of the 6ϕ term will begin to increase toward zero again. It is possible, however, that another gap symmetry will emerge as this happens.[20]

The behavior of the $\cos(10\phi)$ coefficient follows a similar pattern to that of $\cos(6\phi)$, including the initial increase in amplitude, while the 14ϕ and 18ϕ terms first decrease and then increase. This can be understood as well on the basis of the motion of the hot spots from the positive regions of the harmonic to the negative regions. It is evident from the plot that, as the harmonic order increases, the minimum of the coefficient occurs at lower chemical potential. This is sensible, for as the first node of the harmonic moves closer to $\phi=0$, the hot spot passes this point more quickly, driving the coefficient negative, but then also reaches the next nodal point more quickly, driving the coefficient back into the positive regime.

D. Temperature effects

The results presented above were all performed at zero temperature, and the question naturally arises: Does the shape of the gap function evolve with temperature? At first glance the temperature dependence of the gap would seem to be largely an overall scale effect due to the thermal $\tanh(\beta E_k/2)$ factor in the gap equation, and for most of the scenarios studied the gap shape does not change significantly with temperature. However, there is one situation, relevant to the electron-doped cuprate NCCO,[30] in which some temperature effects do exist. Figure 5 plots normalized gap functions at increasing temperature for the chemical potential $\mu=-0.4$, corresponding to an electron-doped cuprate. Here ξ_{AFM}/a was taken as 20. At relatively large antiferromagnetic correlation lengths, as observed in Ref. 30, the peak in the gap function becomes slightly narrower as temperature increases, which is rather surprising as one generally expects increasing temperature to smear out features in gap spectra. This, however, can be explained as follows: the thermal factor $\tanh[\beta/2\sqrt{(\epsilon_k-\mu)^2+\Delta^2(\mathbf{k})}]$ only acts to limit the gap amplitude in those regions where the quasiparticle energy is significantly less than the temperature. This means that, as the temperature increases, the small-$\Delta(\mathbf{k})$ regions are suppressed more than the rest of the gap function, whose energy is larger. This is exactly the behavior demonstrated in Fig. 6.

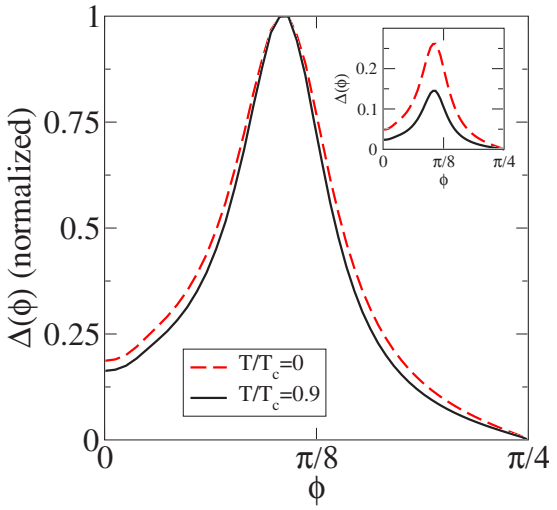

FIG. 6. (Color online) Narrowing of the gap function with increasing temperature.

E. Impurity scattering effects

One important point regarding the gap functions presented in the previous plots is that while the qualitative evolution of the gap functions with doping is consistent with the experimental data, the gap functions for the $\mu=-1.2$ case are much shallower near the nodal region than those observed in experiment.[15,16] This form is only weakly dependent on correlation length, as shown earlier, and we must therefore consider possible alternative explanations, such as impurity scattering, for the differences between theory and experiment.

Impurity scattering would generally be expected to weaken the effect of the DOS singularity at the Van Hove point $(\pi,0)$ by introducing an additional self-energy component to the dispersion, so that the quasiparticle energy at the

Van Hove point, relative to the chemical potential, is increased slightly. This effect is expected to be stronger at the Van Hove point than at the nodal point due to the much larger Fermi velocity near the nodal point, so that the self-energy effect is comparatively smaller. (We have here neglected the self-consistent calculation of the Fermi surface with the modified dispersion.)

We take here the Born and unitary limits for isotropic, s-wave scattering, within which the quasiparticle energy ω is renormalized to $\tilde{\omega}$ as follows:[31]

$$\tilde{\omega} = \omega + \Gamma \left\langle \frac{\tilde{\omega}}{\sqrt{\tilde{\omega}^2 + \Delta(k)^2}} \right\rangle_{FS}^{\pm 1}. \quad (14)$$

The + sign is for the Born limit, while the − sign is the unitary limit. The integral is taken over the Fermi surface, and $\Gamma = n_i/\pi N_0$, with n_i the impurity concentration and N_0 the normal-state density of states. In practice, the second term on the right-hand side of this equation is the self-energy resulting from the impurity scattering and is added to the quasiparticle energy in the dispersion. Therefore, we have solved this equation self-consistently with the gap equation, as follows:

$$\Delta(\mathbf{k}) = \int g \frac{d^2\mathbf{k}'}{(2\pi)^2} [\chi(\mathbf{k}-\mathbf{k}')] \tanh(E_{k'}/2T) \frac{\Delta(\mathbf{k}')}{2E_{k'}} \quad (15)$$

where $E_{k'} = \sqrt{[\varepsilon_{k'} - \mu + \Sigma(\varepsilon_{k'})]^2 + \Delta^2(\mathbf{k}')}$, where $\Sigma(\varepsilon_{k'})$ is the self-energy for $\varepsilon_{k'} = \omega$. In Fig. 7 we present a calculation of the effects of impurity scattering on gap shape at a few impurity scattering levels, for $\mu = -1.2$ and $\xi/a = 5$. Within this approximation, in both the Born and unitary limits, impurity scattering is seen to have a negligible impact on gap symmetry (it does significantly decrease gap amplitude, which is shown in the inset) This is due to the relatively small size of the impurity energy scale[32] ($\sim\sqrt{\Gamma\Delta} \sim 0.05t$) involved relative to t. If the strength of the superconducting pairing is increased substantially and the impurity concentration is also increased, significantly stronger gap symmetry changes emerge. This, however, produces unrealistically high transition temperatures of the order of $0.1t$, or 400 K (taking t as 0.35 eV), and so we think it unlikely that impurity scattering is responsible for the primarily concave $\cos(2\phi)$ shape of the order parameter observed in cuprates. From an experimental point of view, it is likely that s-wave impurity-doped cuprates have essentially the same gap symmetry as the pure-case material. ARPES measurements would be most useful in this regard.

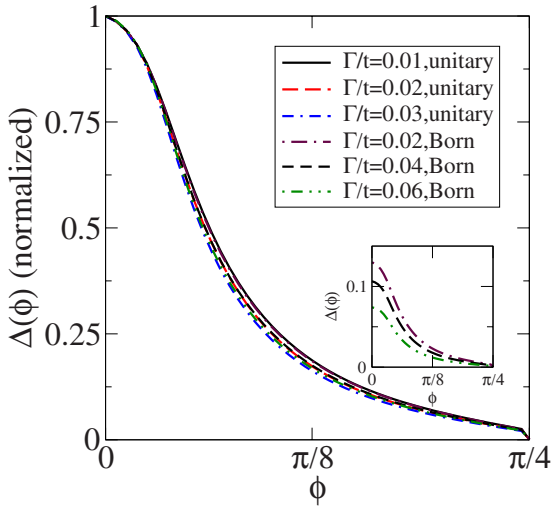

FIG. 7. (Color online) Effect of impurities on gap symmetry, for $\mu = -1.2$ ($n_h = 0.3$) and $\xi/a = 5$. Inset: Unnormalized gap functions.

IV. SUMMARY

In this paper, we have presented the effects of correlation length, doping, temperature, and impurity scattering on order parameter symmetry in the high-T_c cuprates. We have found that within a two-dimensional spin-fluctuation model the gap symmetry is essentially independent of correlation length. We find good quantitative agreement with experiment for the proportion of the first d-wave harmonic, $\cos(6\phi)$, in the solution to the generalized gap equation. We observe a slight but unusual dependence of gap symmetry on temperature for the electron-doped cuprates. Finally, we find little effect of impurity scattering, in either the Born or unitary limit, on gap symmetry.

ACKNOWLEDGMENTS

S.H. acknowledges the support of the Petroleum Energy Research Fund. A.B. acknowledges the support of the U.S. Department of Energy. D.P. is pleased to acknowledge several useful discussions with Ilya Eremin and valuable interaction with Andrey Chubukov.

[1] D. A. Brawner and H. R. Ott, Phys. Rev. B **50**, 6530 (1994); **53**, 8249 (1996); A. Mathai, Y. Gim, R. C. Black, A. Amar, and F. C. Wellstood, Phys. Rev. Lett. **74**, 4523 (1995).

[2] C. C. Tsuei, J. R. Kirtley, C. C. Chi, Lock See Yu-Jahnes, A. Gupta, T. Shaw, J. Z. Sun, and M. B. Ketchen, Phys. Rev. Lett. **73**, 593 (1994); C. C. Tsuei, J. R. Kirtley, M. Rupp, J. Z. Sun, A. Gupta, M. B. Ketchen, C. A. Wang, Z. F. Ren, J. H. Wang, and M. Bhushan, Science **271**, 329 (1996); J. R. Kirtley, C. C. Tsuei, J. Z. Sun, C. C. Chi, Lock See Yu-Jahnes, A. Gupta, M. Rupp, and B. Ketchen, Nature (London) **373**, 225 (1996).

[3] W. N. Hardy, D. A. Bonn, D. C. Morgan, Ruixing Liang, and Kuan Zhang, Phys. Rev. Lett. **70**, 3999 (1993); W. N. Hardy, S. Kamal, D. A. Bonn, K. Zhang, R. Liang, E. Klein, D. C. Morgan, and D. J. Baar, Physica B **197**, 609 (1994); K. A. Moler, D. J. Baar, J. S. Urbach, Ruixing Liang, W. N. Hardy, and A. Kapitulnik, Phys. Rev. Lett. **73**, 2744 (1994).

[4] C. Renner and O. Fischer, Phys. Rev. B **51**, 9208 (1995); M. Oda, C. Manabe, and M. Ido, *ibid.* **53**, 2253 (1996).

[5] T. E. Mason, G. Aeppli, and H. A. Mook, Phys. Rev. Lett. **68**, 1414 (1992); T. E. Mason, G. Aeppli, S. M. Hayden, A. P. Ramirez, and H. A. Mook, *ibid.* **71**, 919 (1993).

[6] J. Y. T. Wei, N.-C. Yeh, D. F. Garrigus, and M. Strasik, Phys. Rev. Lett. **81**, 2542 (1998); G. Deutscher, Rev. Mod. Phys. **77**, 109 (2005).

[7] C. C. Tsuei, J. R. Kirtley, G. Hammerl, J. Mannhart, H. Raffy, and Z. Z. Li, Phys. Rev. Lett. **93**, 187004 (2004).

[8] We note that while predominant *d*-wave symmetry is firmly established for the hole-doped cuprates, there is still some doubt regarding some electron-doped cuprates, which do not commonly show the zero-bias conductance peak (Ref. 9) expected for *d*-wave symmetry. There is also evidence for a nonmonotonic *d*-wave symmetry from Raman scattering (Ref. 10) in electron-doped cuprates, and some indications for the same in hole-doped cuprates (Ref. 11).

[9] I. Eremin (private communication).

[10] G. Blumberg, A. Koitzsch, A. Gozar, B. S. Dennis, C. A. Kendziora, P. Fournier, and R. L. Greene, Phys. Rev. Lett. **88**, 107002 (2002).

[11] O. V. Misochko and E. Ya Sherman, J. Phys.: Condens. Matter **12**, 9095 (2000).

[12] S. Haas, A. V. Balatsky, M. Sigrist, and T. M. Rice, Phys. Rev. B **56**, 5108 (1997).

[13] H. Ghosh, Phys. Rev. B **60**, 6814 (1999).

[14] Y. Bang, I. Martin, and A. V. Balatsky, Phys. Rev. B **66**, 224501 (2002).

[15] S. V. Borisenko, A. A. Kordyuk, T. K. Kim, S. Legner, K. A. Nenkov, M. Knupfer, M. S. Golden, J. Fink, H. Berger, and R. Follath, Phys. Rev. B **66**, 140509(R) (2002).

[16] J. Mesot, M. R. Norman, H. Ding, M. Randeria, J. C. Campuzano, A. Paramekanti, H. M. Fretwell, A. Kaminski, T. Takeuchi, T. Yokoya, T. Sato, T. Takahashi, T. Mochiku, and K. Kadowaki, Phys. Rev. Lett. **83**, 840 (1999).

[17] S. I. Vedeneev and D. K. Maude, Phys. Rev. B **72**, 144519 (2005).

[18] M. Chiao, R. W. Hill, C. Lupien, L. Taillefer, P. Lambert, R. Gagnon, and P. Fournier, Phys. Rev. B **62**, 3554 (2000).

[19] P. Monthoux, A. V. Balatsky, and D. Pines, Phys. Rev. Lett. **67**, 3448 (1991); Phys. Rev. B **46**, 14803 (1992); P. Monthoux and D. Pines, Phys. Rev. Lett. **69**, 961 (1992).

[20] V. A. Khodel, V. M. Yakovenko, M. V. Zverev, and H. Kang, Phys. Rev. B **69**, 144501 (2004).

[21] J. Bardeen, L. N. Cooper, and J. R. Schrieffer, Phys. Rev. **108**, 1175 (1957).

[22] D. Manske, I. Eremin, and K. H. Bennemann, Phys. Rev. B **67**, 134520 (2003).

[23] A. Ino, C. Kim, M. Nakamura, T. Yoshida, T. Mizokawa, A. Fujimori, Z.-X. Shen, T. Kakeshita, H. Eisaki, and S. Uchida, Phys. Rev. B **65**, 094504 (2002).

[24] J. H. Ngai, W. A. Atkinson, and J. Y. T. Wei, Phys. Rev. Lett. **98**, 177003 (2007).

[25] H. J. H. Smilde, A. A. Golubov, Ariando, G. Rijnders, J. M. Dekkers, S. Harkema, D. H. A. Blank, H. Rogalla, and H. Hilgenkamp, Phys. Rev. Lett. **95**, 257001 (2005).

[26] J. R. Kirtley, C. C. Tsuei, A. Ariando, C. J. M. Verwijs, S. Harkema, and H. Hilgenkamp, Nat. Phys. **2**, 190 (2006).

[27] M. A. Kastner, R. J. Birgeneau, G. Shirane, and Y. Endoh, Rev. Mod. Phys. **70**, 897 (1998).

[28] D. Manske, I. Eremin, and K. H. Bennemann, in *The Physics of Superconductors*, edited by K. H. Benneman and J. B. Ketterson (Springer, Berlin, 2004), Vol. 2.

[29] H. Matsui, K. Terashima, T. Sato, T. Takahashi, M. Fujita, and K. Yamada, Phys. Rev. Lett. **95**, 017003 (2005).

[30] E. M. Motoyama, G. Yu, I. M. Vishik, O. P. Vajk, P. K. Mang, and M. Greven, Nature (London) **445**, 186 (2007).

[31] A. A. Abrikosov and L. P. Gorkov, Sov. Phys. JETP **12**, 1243 (1961).

[32] H. Won, S. Haas, D. Parker, S. Telang, A. Vànyolos, and K. Maki, in *Lectures on the Physics of Highly Correlated Electron Systems IX*, edited by A. Avella and F. Mancini, AIP Conf. Proc. No. 789 (AIP, Melville, NY, 2005), pp. 3–43.